International Journal of Impact Engineering 173 (2023) 104474

Contents lists available at ScienceDirect

International Journal of Impact Engineering

journal homepage: www.elsevier.com/locate/ijimpeng

Simplified model to consider influence of gravity on impacts on structures: Experimental and numerical validation

Javier Sánchez-Haro, Ignacio Lombillo *, Guillermo Capellán

Department of Mechanical and Structural Engineering, University of Cantabria, Av. de los Castros 44, 39005, Santander Spain

ARTICLE INFO

Keywords:
Impact
Contact force
Gravitational influence
Experimental test

ABSTRACT

Traditionally, the effect of gravitational force has not been considered in the study of impacts on structures, partly due to lack of knowledge. In most cases, it may be reasonable to disregard this effect, but it is not clear where the limit is and, therefore, in which cases its effect should be considered. Is this limit the same regardless of the type of structure? What criterion should be adopted? This paper develops a simplified model that allows, through a simple formulation, the calculation of the displacement and contact force in an impact considering the effect of the force of gravity on the structural response. In this article, the formulation has been validated with experimental impact tests on beams and also with finite element models. In addition, a coefficient is proposed which enables the evaluation, prior to any analysis, of whether the impact will be significantly influenced by the force of gravity, whatever the structure under study.

Definitions

A	Area of cross section
$A_{G,\,t}$	Amplitude of gravitational term at time t
$A_{K,\,t}$	Amplitude of Kinetic term at time t
C_{sw}	Self-Weight Coefficient. Amplitude ratio between gravitational and kinetic terms at $T_{sp}/4$
$D_p(t)$	Projectile displacement at time t
$D_s(t)$	Structure displacement at time t
E	Elastic modulus
F(t)	Contact force between projectile and structure at time t
g	Gravity acceleration
H_0	Height where the projectile is dropped
I	Moment of Inertia
K_s	Equivalent stiffness of the structure of the fundamental mode of vibration
L	Length of the structure
M_s	Equivalent mass of the structure of the fundamental mode of vibration
M_p	Mass of the projectile
t	Time instant
t_f	Instant when the projectile stops and at which the maximum displacements occur
t_0	Instant when the impact begins
T_{sp}	Period of vibration related with W_{sp}
V_I	Velocity of the projectile and structure the instant just after impact.
$V_{p,0}$	Velocity of the projectile the instant just before impact
$V_p(t)$	Velocity of the projectile at time t
W_s	Frequency of vibration of the fundamental mode of the structure
W_{sp}	Frequency of vibration of the fundamental mode of the structure during projectile impact
y	Variable of integration
α	Mass ratio between projectile and structure
ρ	Density

1. Introduction

For high impact velocities, it is intuitively understood that the effect of gravity will not affect the structural response. For example, if a bullet hits a beam, the effect will be the same whether it hits in the direction of gravity or in the direction perpendicular to gravity. However, this is not true for low impact velocities. For example, if a heavy rock is dropped from a minimal height the rock will impact the structure only if the direction of impact is in the direction of gravity, as it will be accelerated against the structure. If it is in the direction perpendicular to gravity, since the pre-impact velocity is zero, the impact will not occur. The two

* Corresponding author.
E-mail address: ignacio.lombillo@unican.es (I. Lombillo).

https://doi.org/10.1016/j.ijimpeng.2022.104474
Received 30 March 2022; Received in revised form 26 October 2022; Accepted 13 December 2022
Available online 14 December 2022

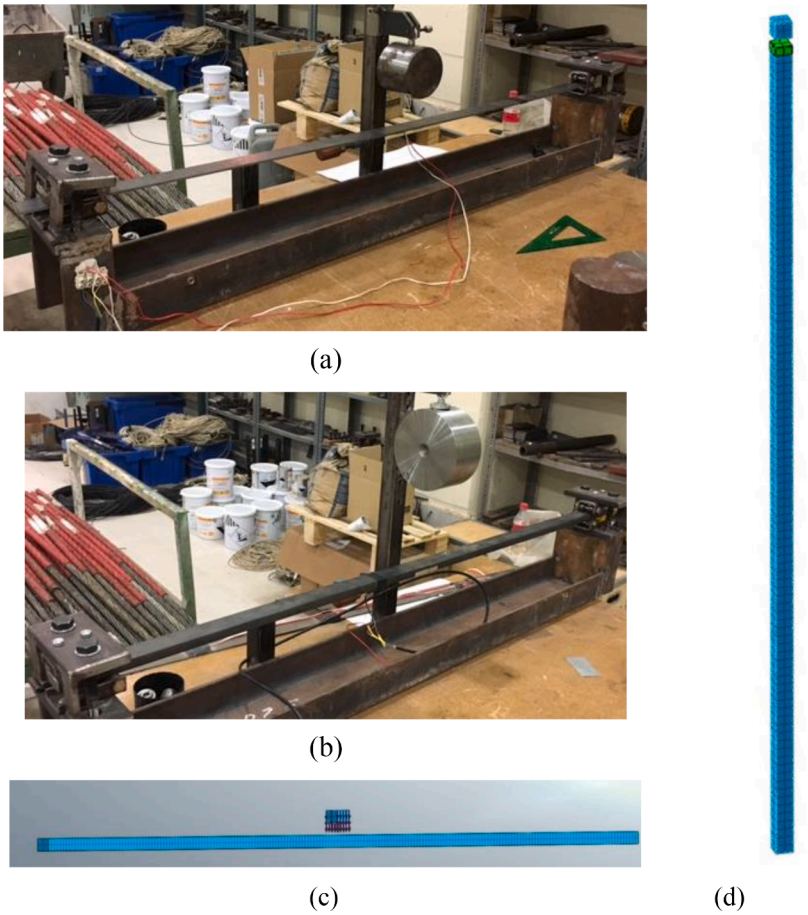

Fig. 1. Definition of the structures studied. **(a)** Beam 1: Simply supported steel beam 1 m long and 0.03 × 0.003 m^2 cross section. **(b)** Beam 2: Simply supported steel beam 1 m long and 0.03 × 0.012 m^2 cross section. **(c)** Beam 3: Simply supported steel beam 10 m long and 0.1 × 0.1 m^2 cross section. **(d)** Column: Fixed bar 5 m long and 0.1 × 0.1 m^2 cross section.

extremes above are clear, but when and how is the limit established? When should the action of gravity be considered to cease to have an effect? Does it affect all structures equally? The following is a brief summary of the development throughout history of impacts on structures, and as can be seen, practically no reference to the influence of gravitational force has been found. The books that compile the main theories [1,2] on impacts scarcely describe any consideration of the effect that the force of gravity can have on impacts. The Cox equation, which only presents results of maximum displacements (not time vs displacement, or time vs contact force histograms), does not approximate real test results well [3–5]. General Classical theories, such as Saint-Venant's theorem [6], or local theories such as Hertz's theory [7], do not consider the possible influence of gravity on the results. Not even the expression obtained by Timoshenko [8], one of the most widely used and still considered a reference, takes it into account. The main problem of Timoshenko's theory is its complexity of application, so that several theories have arisen trying to simplify it [9,10]. In any case, none of these proposals of simplifications of Timoshenko's theory included the effect of gravity on the structural response.

Lee [11] in 1940 or Lee, Hamilton and Sullivan [12], who developed simplified methods (one-degree-of-freedom, 1DoF) to solve the impact, did not consider the effect of gravity in their calculations.

The classical simplified 2DoF models, which also considered the local deformation of the structure or the projectile, did not introduce any mention of the force of gravity in their expressions either. Examples include Suaris and Shah's model [13] or Shivakumar, Elver and Illg's model [14]. In the quest to gain accuracy and applicability, 2DoF models have continued to be developed up to the present day with the continuous intention of simplifying and better understanding impacts, improving on the previous models [15–17]. However, there is no special reference to the effect of gravity due to vertical impact in [15] regarding [16,17] where horizontal impacts occurs.

Current multi-degree-of-freedom models are not so focused on simplification, but rather on reducing the calculation times of commercial software. Some examples of this include S. Shi, L. Zhu, and T. X. Yu's analytical model [18] in which the impact is perpendicular to the direction of gravity and thus the influence of gravity can be avoided or the mixed models (analytical + local FEM model) of Q. Hao [19] where the impact occurs parallel to the direction of gravity. This last model was also developed without considering the effect of the gravitational force on impacts. This lack is not only found in the transverse impacts on beams referenced previously, but also in the case of other types of impacts, such as longitudinal impacts on bars in the vertical direction [20] where there is no special mention of the effect of gravity with respect to longitudinal impacts on bars in the horizontal direction [21,22]. In the cases of transverse impacts on plates in a vertical direction [23,24], the influence of gravity in calculations was not taken into account.

Nowadays, impacts are still under study by means of alternative models to FEM ones due to the problems of cost in calculation time, convergence, or verification of results. These focus on both classic materials [25,26], and on new materials [27–29], but in no case is the possible influence of the force of gravity considered despite all of them being vertical impacts (i.e. parallel to the direction of gravity). Furthermore, several experimental tests were carried out where a mass was dropped from a height onto different beams [30–33] and all of them were analysed without considering the effect of gravity. Is this common

Table 1
Definition of structural and impact parameters in each case.

Case study	Struct.	K_s (N/m)	M_s (kg)	W_s (Rad/s)	M_p (kg)	α (M_p/M_s)	W_{sp} (Rad/s)	H_0 (m)	$V_{p,0}$ (m/s)
1	Beam1	680	0.353	43.89	2.55	7.2	15.30	0.000	0.00
2	(B1)							0.022	0.66
3								0.096	1.37
4	Beam2	43,546	1.413	175.55	5.00	3.5	82.40	0.010	0.43
5	(B2)							0.037	0.85
6								0.110	1.47
7	Beam3	84,000	392.500	14.63	1177.50	3.0	7.31	0.001	0.14
8	(B3)							0.100	1.40
9								1.275	5.00
10								5.099	10.0
11	Column (C)	420,000	159.360	51.34	1593.60	10.0	15.49	0.005	0.31

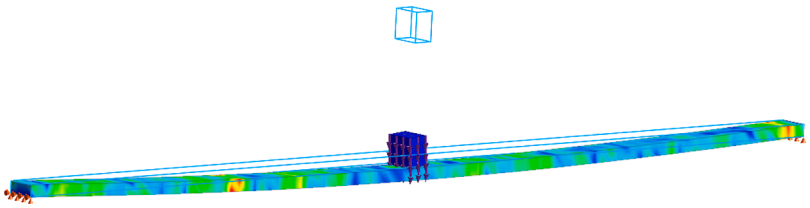

Fig. 2. Sketch of FEM model.

Table 2
FEM model definition.

Structure		Length (m)	Width (m)	Height (m)	No elements	E (kN/m^2)	Density (kg/m^3)
B1	Beam mesh size	0.010	0.010	0.003	300	2.1e08	7850
	Projectile dimensions	0.020	0.030	0.030	18	1.0e15	141,666
B2	Beam mesh size	0.010	0.010	0.012	300	2.1e08	7850
	Projectile dimensions	0.020	0.030	0.030	18	1.0e15	277,777
B3	Beam mesh size	0.050	0.050	0.050	800	2.1e08	7850
	Projectile dimensions	0.100	0.100	0.100	8	1.0e15	1177,500
C	Column mesh size	0.050	0.050	0.050	400	2.1e05	7850
	Projectile dimensions	0.100	0.100	0.100	8	1.0e15	1590,000

Fig. 3. **(a)** Data logger NI-PXI e 1078. **(b)** Data display screen.

assumption adequate for vertical impacts like those? The last four articles were analysed with the formulation proposed in this research. The error due to the unconsidered force of gravity is less than 3.5%, so the assumption is correct. That is so because the beams subjected to impact are rigid. However, the gravity effect may not be negligible, as will be shown later, considering other stiffness values and different impact velocities. The specific properties of the collision must be checked to avoid significant errors due to not taking into account the force of gravity. In order to contribute to the clarification of this matter, this article enables the effect of the force of gravity to be considered in a simplified model for any structure based on a previous simplified model [34] that does not consider the effect of gravity. However, this research

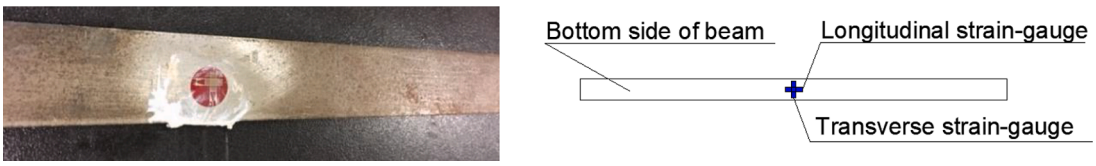

Fig. 4. Bidirectional strain-gauge model Tokyo Sokki FCA-3–11–1L.

Fig. 5. Potentiometer displacement transducer unit (Penny Giles, SLS095 model).

was limited to impact on beams in order to simplify experimental test campaigns. Ten different impact cases were analysed in this article with different degrees of influence of the force of gravity. Six of them were experimental tests on two beams of small dimensions and four were numerical tests on larger beams. The experimental tests were used to check both the FEM results and the proposed formulation. Once it was verified that the results of the FEM models match well with the experimental results, the four numerical tests were carried out using only the FEM model. All of them were compared with the results obtained from the proposed formulation with good results. This article is organised as follows. The introduction sets out the general background and the main objectives In the "Material and Methods" section, the eleven scenarios (case studies) analysed are presented, explaining the equivalent stiffness and equivalent mass of the structure in each case. Then, FEM models are described that provide sufficient details to enable any researcher to reproduce the ten cases studied. The last part of this section describes the measurement system used to obtain the data from the experimental tests. In the next section "The theoretical basis of the simplified model" for general impact considering gravitational influence is introduced, obtaining the proposed formulation used to calculate the impact force and the displacement produced in the structure. In the "Results" section, results are presented and validated by means of finite element models and experimental tests, and then they are discussed. Finally, the main conclusions drawn in the investigation are highlighted.

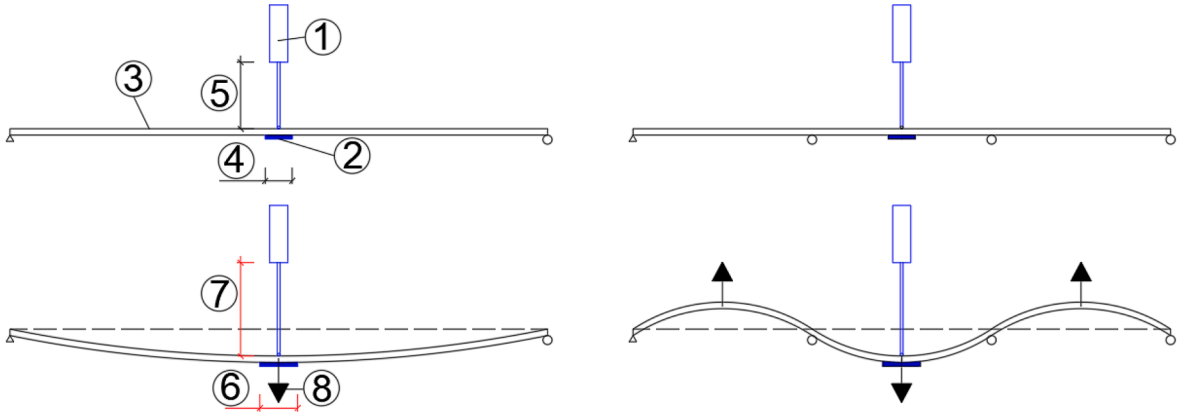

Fig. 6. Sketch of static test for calibration of the strain-gauge. Mode 1(left). Mode 3 (right). (1) PDTU. (2) Strain-gauge. (3) Beam. (4) Initial length of strain-gauge. (5) Initial length of PDTU. (6) Final length of strain-gauge. (7) Final length of PDTU. (8) Applied force in static test.

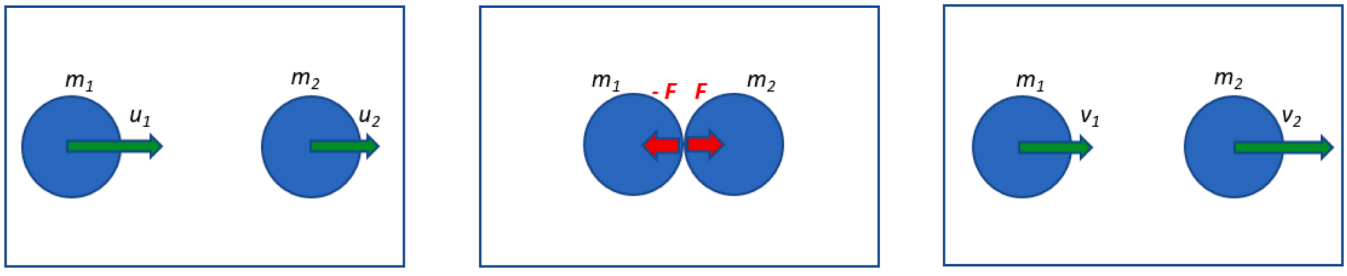

Fig. 7. Classic impact of co-linear masses.

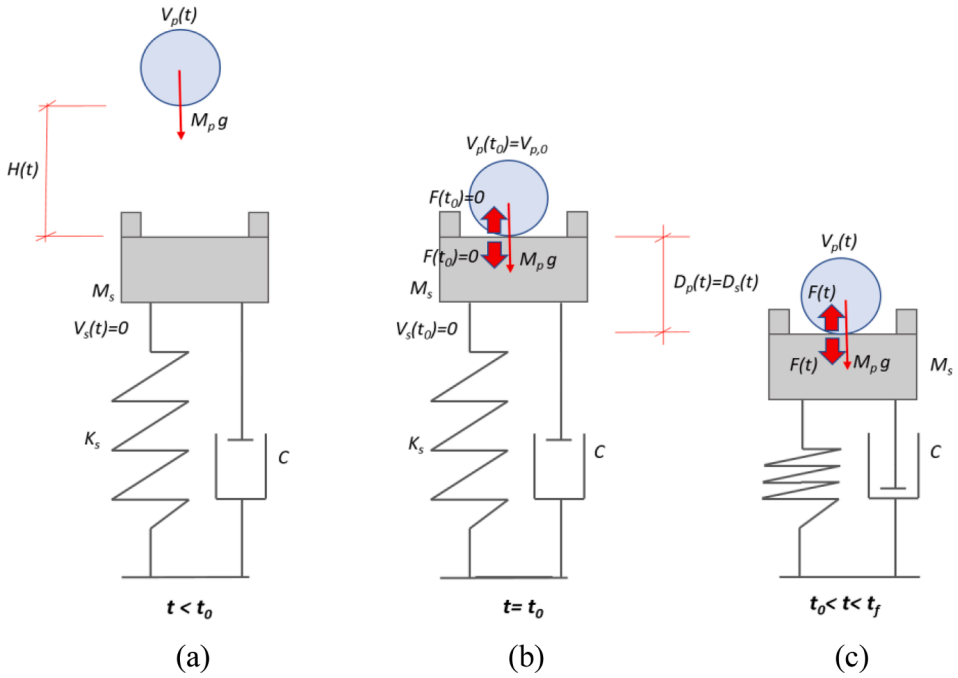

Fig. 8. Idealized impact sequence. **(a)** Situation before the impact between the projectile and the structure. **(b)** Instant of impact ($t = t_0$). **(c)** Situation between the beginning and the end of the impact ($t_0 < t < t_f$).

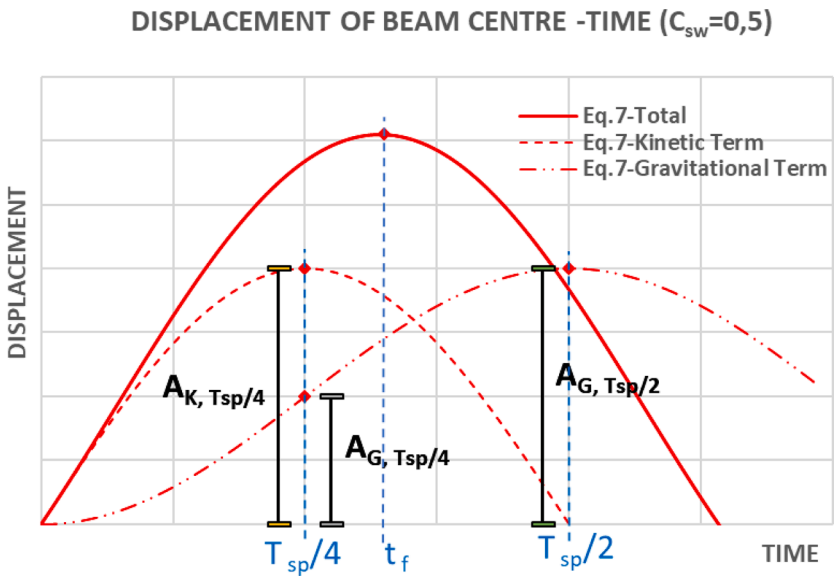

Fig. 9. Example of a self-weight coefficient (C_{sw}) = 0.5.

2. Materials and methods

2.1. Case studies

The method has a general character, valid for any structure, as any structure can be simplified into a spring-mass system, but in this article it has been applied preferentially to beams because of the ease of testing them in the laboratory. Testing experimental impacts on large beams in the laboratory presents logistical difficulties, so a mixed validation system was used. On the one hand with experimental tests for small beams (Fig. 1a,b) and, on the other, by using FEM models to be able to consider beams of larger dimensions (Fig. 1c) and other different structures such as a column with longitudinal impact (Fig. 1d).

To make the method general, any structure must be transformed into an equivalent 1DoF spring-mass system. In [35] the performance of this step is demonstrated in a simple way for any structure, but it will not be dealt with in this article. For the present case, 3 simply supported beams with transverse impacts at the centre and a column with longitudinal impact at the free edge were studied. In [35], it was demonstrated that the spring stiffness can be obtained from the expression: $K_s = 48\mathrm{EI}/L^3$ for beams and $K_s = \mathrm{EA}/L$ for the column. In the same reference, in an analogous way, it is shown that the effective mass for the same assumption is half of the total mass for beams $M_s = 0.5M_{Total}$ and $M_s = 0.4M_{Total}$ for the column. The frequency of the fundamental mode of vibration of the spring-mass system, W_s, and the frequency of the fundamental mode of vibration during impact W_{sp} (which means considering the projectile mass M_p as a structural mass [34]), can be

Table 3
Maximum displacement of the structure obtained by means of the proposed formulation, FEM model or experimental tests.

Case	Type	Struc-ture	W_{sp} (Rad/s)	C_{sw}	$D_s(t)_{max,\ Eq.\ (7)}$ (m)	$D_s(t)_{max,\ Test}$ (m)	$D_s(t)_{max,\ FEM}$ (m)	$D_s(t)_{max,\ Error}$ (%)
1	Test	B1	15.30	∞	7.35e-2	7.22e-2	7.35e-2	1.9*
2				0.98	8.94e-2	08.94e-2	8.76e-2	1.2*
3				0.47	1.24e-1	1.26e-1	1.20e-1	2.1*
4	Test	B2	82.40	0.28	5.36e-3	5.32e-3	5.37e-3	0.7*
5				0.14	9.26e-3	9.53e-3	9.03e-3	2.8*
6				0.08	1.51e-2	1.57e-2	1.46e-2	3.8*
7	FEM	B3	7.31	9.58	2.72e-1	–	2.75e-1	1.4**
8				0.96	3.32e-1	–	3.32e-1	0.0**
9				0.27	6.62e-1	–	6.49e-1	2.0**
10				0.13	1.15e0	–	1.11e0	4.2**
11		C	15.49	2.00	7.85–2	–	8.60e-2	8.7**
					$\mathbf{F}(t)_{max,\ Eq.\ (8)}$ (kN)	$\mathbf{F}(t)_{max,\ Test}$ (kN)	$\mathbf{F}(t)_{max,\ FEM}$ (kN)	$\mathbf{F}(t)_{max,\ Error}$ (%)
					3.45e1	–	3.12e1	9.4**

* Relative error calculated based on the ratio between experimental test and the proposed formulation.
** Relative error calculated based on the ratio between FEM and the proposed formulation.

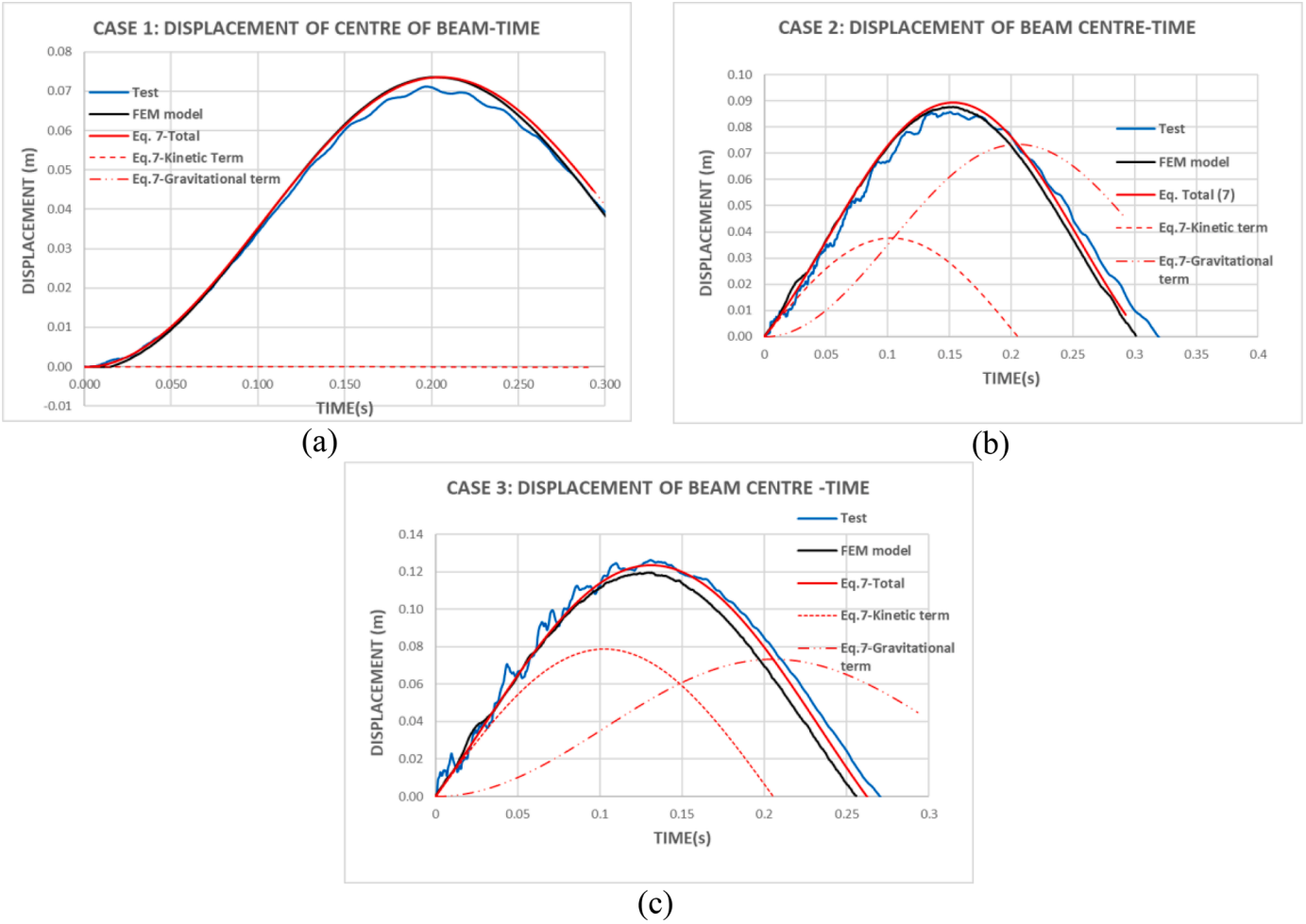

Fig. 10. Comparison of results for beam 1. **(a)** Case 1 ($C_{sw} = \infty$). **(b)** Case 2 ($C_{sw} = 0.98$). **(c)** Case 3 ($C_{sw} = 0.47$).

obtained from the expressions $W_s = \sqrt{K_s/M_s}$ and $W_{sp} = \sqrt{\frac{K_s}{M_s+M_p}}$. The values of K_s, M_s, W_{sp} and W_s of the three beams under study are shown in Table 1. The parameters defining the impact in each case are defined next. The mass ratio between projectile and structure defines the parameter $\alpha = M_p/M_s$. High values of α were chosen because this is where the effect of the projectile's self-weight is most likely to have the greatest influence. On the other hand, as discussed in [34], values of this parameter higher than 1 ensure that the fundamental mode of vibration is the main one involved in the impact, which means that the impact energy is absorbed mainly by the fundamental mode. The first 10 cases were defined to check the proposed formulation regarding displacements. As far as contact forces are concerned, in transverse impacts such as those exerted in cases 1 – 10 of this article, the contact force can be estimated from the shear forces. However, finite element models do not

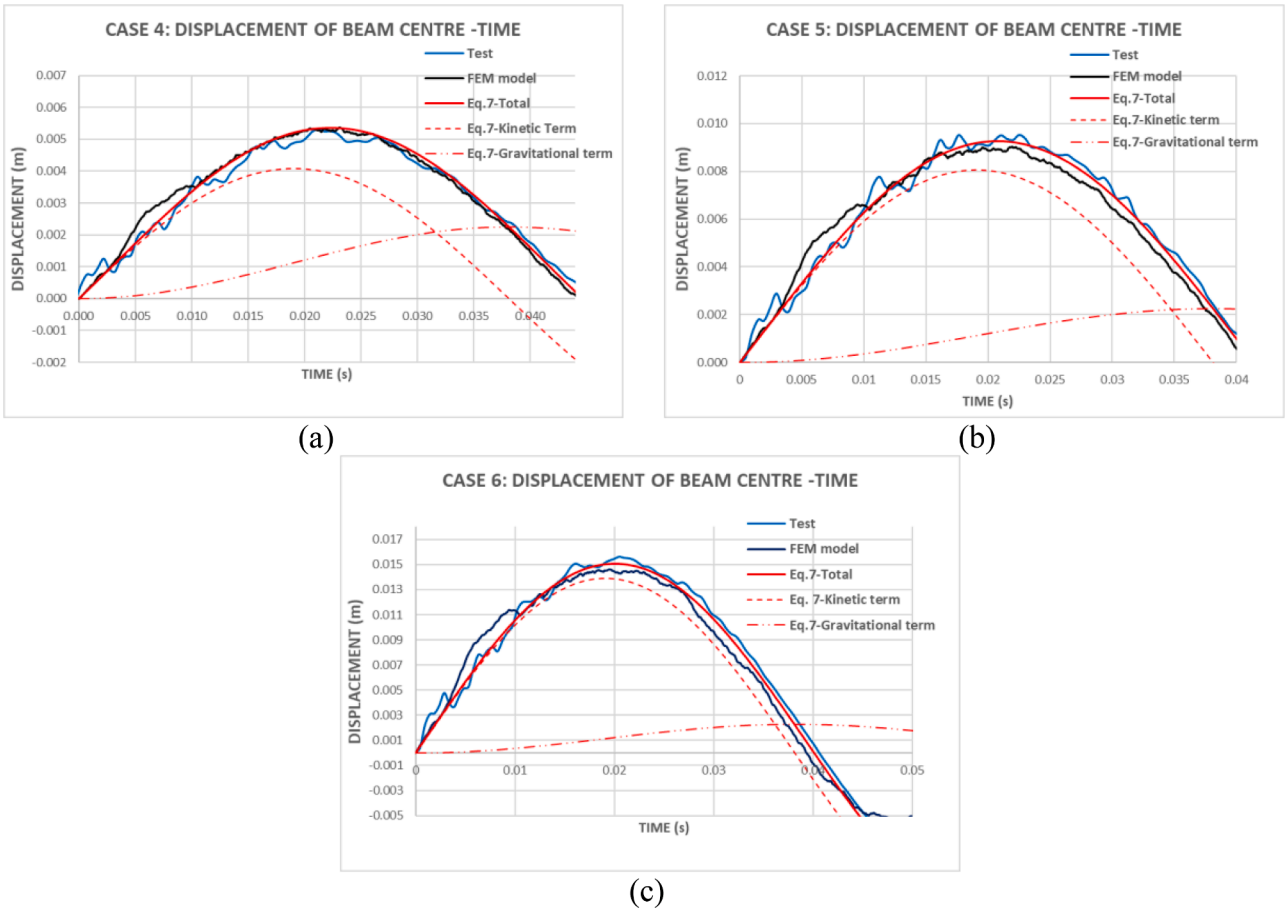

Fig. 11. Comparison of results for beam 2. **(a)** Case 4 (C_{sw} = 0.28). **(b)** Case 5 (C_{sw} = 0.14). **(c)** Case 6 (C_{sw} = 0.08).

provide sufficient accuracy for modelling because, due to the thin plate theory of the finite element method, the error increases with each derivation step, which in practice makes it impossible to obtain the contact force accurately from the shear forces [36,37]. This is the reason why case 11 is analysed, where a longitudinal impact is exerted instead of a transverse one, as in that situation the contact forces can be obtained with sufficient accuracy from the axial forces due to the lower order of derivation.

Different projectile drop heights H_0 were considered, which defines the projectile velocity at the instant before impact $V_{p,0}$ according to the well-known expression $V_{p,0} = \sqrt{2gH_0}$. The values of α, H_0 and $V_{p,0}$ for the 11 cases analysed in this article are shown in Table 1.

2.2. Description of the models in Midas NFX

For each case, the structure was modelled in Midas NFX through finite solid elements, defining a contact without friction between bodies and using a nonlinear explicit transient analysis type, Fig 2.

The projectile was given small dimensions so as to act as a point mass. The mesh size of the structure, the projectile dimensions, and the elastic moduli and densities for each case, are compiled in Table 2. In order to reproduce the hypothesis of an infinitely rigid projectile, its elastic modulus E was set to 1e15 kN/m^2. Mesh size was modified in order to ensure no influence on results. The time increment used for numerical integration in Midas NFX was 1e-4 s for beam 1 and 3 and it was 1e-5 s for beam 2. This time increment ensures more than 1000 data before maximum displacement of the test. It was also verified that smaller time increments produce the same results, so results converged.

Constant nodal forces were applied in all the projectile nodes in order to simulate the acceleration due to gravity. The total gravity force on the projectile is different in each case depending on the mass of the projectile but it is applied in such a way that a total constant acceleration of the projectile equal to 9.8 m/s^2 is produced towards the beam direction.

3. Theoretical basis of the simplified model

3.1. Initial hypothesis

Initially, some assumptions must be defined in order to state and solve the problem of impacts on structures. The closer the initial assumptions are to the actual impact conditions, the closer the results of the formulation are to the exact ones. The following is a description of the assumptions adopted. The *structure* is made of a linear elastic material or equivalent if this is required for plastic analysis. The structure is initially at rest, i.e. has no movement. Shear and membrane forces and local deformation have not been considered in the simplified model (however, they have been considered in the FEM model developed). Membrane forces only have an influence when displacements are large, but this is not expected in this kind of structures. Shear forces and local deformation slightly increase the total displacement, so they have some influence depending on the case. However, the aim of the paper is to analyse the impact easily in order to pre-design structures and to check FEM results. Thus, it does not make sense to include them in formulation if the contribution is limited and they do not modify the general behaviour of structures under impact loads. Local and shear deformations are not important from a pre-design or a verification point of view. In any case, the suitability of these hypotheses will be analysed later. The initial velocity of the *projectile* is perpendicular to the structure. The projectile is made of an infinitely rigid material. The projectile has no dimensions what implies that it is supposed to act at a point. The

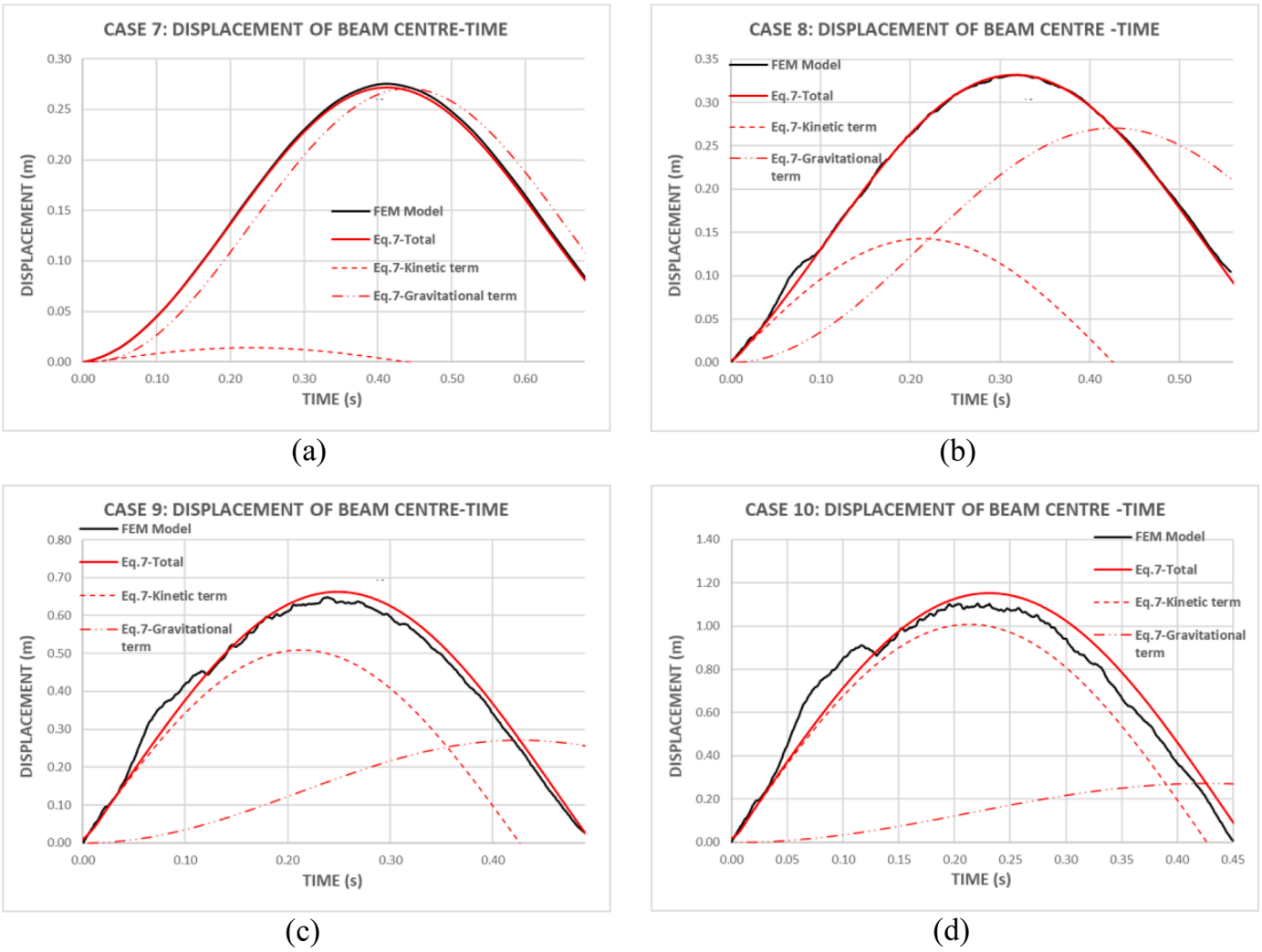

Fig. 12. Comparison of results for beam 3. **(a)** Case 7 (C_{sw} = 9.58). **(b)** Case 8 (C_{sw} = 0.96). **(c)** Case 9 (C_{sw} = 0.27). **(d)** Case 10 (C_{sw} = 0.13).

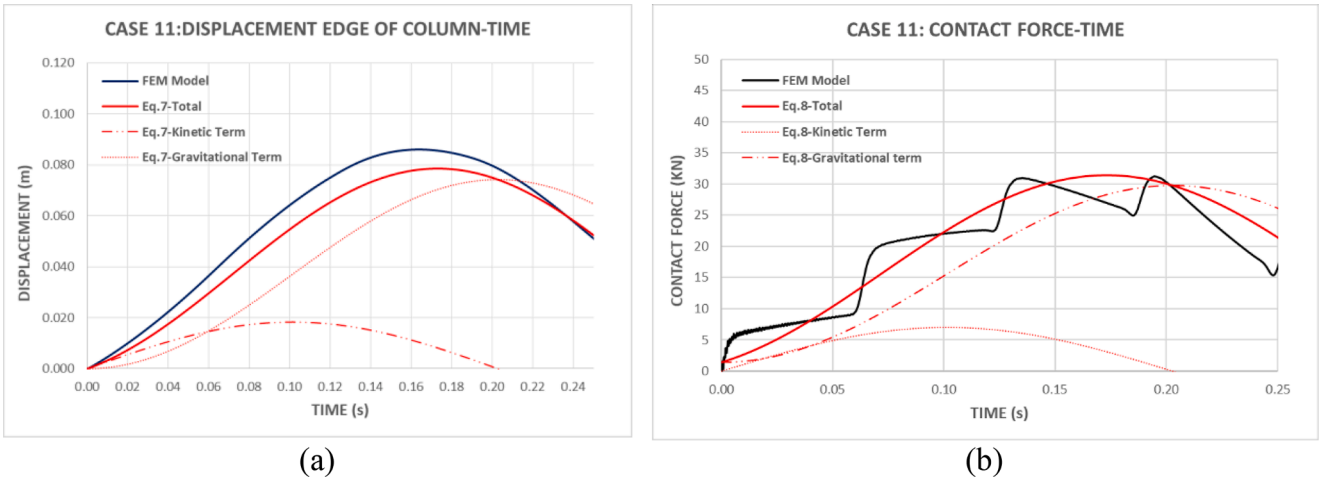

Fig. 13. Comparison of results for column. Case 11 (C_{sw} = 2.00). **(a)** Displacements. **(b)** Contact force.

mass of the projectile is heavier than the effective mass of the structure.

The *impact* is considered of low velocity, that is, viscous behaviour of the materials is excluded. Structural damping was not considered due to the fact that impact duration is too short to allow its development. There are no energy losses due to heat, noise or structural damping during the impact. The impact is centred, that is, the point of contact and the centroids of the projectile and the structure are aligned. The impact begins when the projectile contacts the structure (t_0), and ends when the projectile stops (t_f). This contact is continuous throughout the impact. The fact that the mass of the projectile is greater than the effective mass

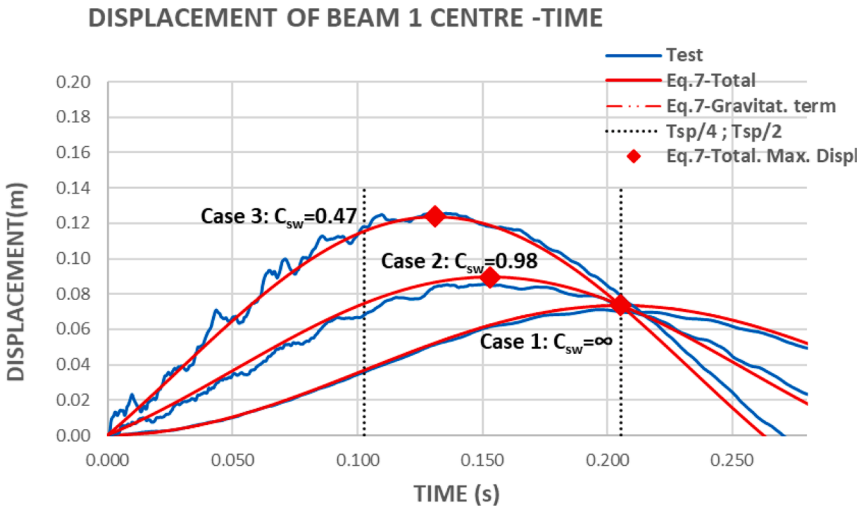

Fig. 14. Combined visualization of cases for beam 1: Cases 1–3.

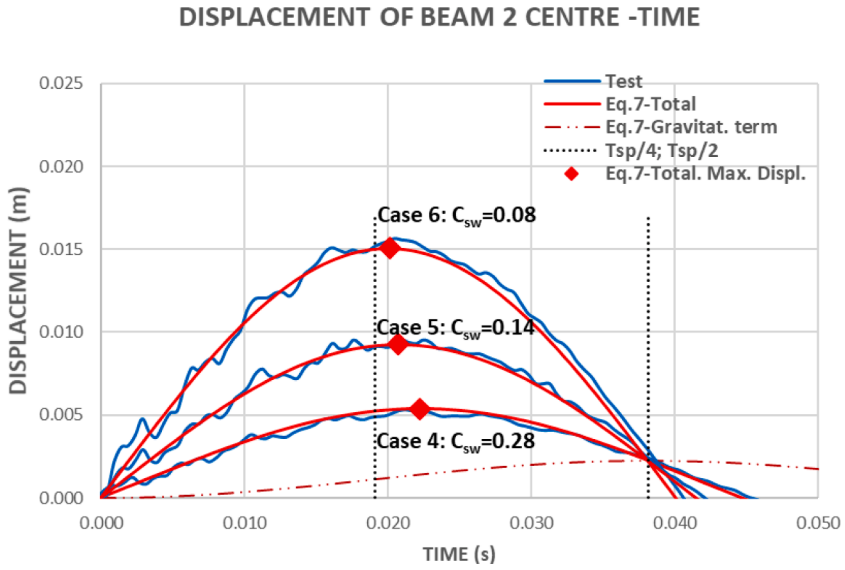

Fig. 15. Combined visualization of cases for beam 2: Cases 4–6.

of the structure means that this assumption is reasonable, since, according to classical impact equations, a light mass cannot stop a heavy one, Fig. 7.

3.2. Problem description

A projectile mass M_p is assumed to have velocity $V_p(t)$ in a perpendicular direction to the structure. The fundamental mode of the structure has an effective mass M_s and an effective stiffness K_s, initially being at rest ($t < t_0$), Fig 8(a). When the impact between the projectile and the structure begins ($t = t_0$), the projectile has a previous impact velocity $V_{p,0}$, the structure remains at rest, and the contact force between the bodies $F(t)$ has not developed yet, and hence its value is null, Fig 8(b). From this point on ($t > t_0$), as a consequence of the impact, the structure deforms at the same time as the projectile's velocity gets reduced. At any moment between the beginning and the end of the impact ($t_0 < t < t_f$), the displacement of the projectile $D_p(t)$ and the structure $D_s(t)$ are the same as a consequence of the initial hypotheses, Fig 8(c). Eqs. (1) and (2) express, respectively, these displacements at time t. The gravitational acceleration g has influence on the projectile during the whole process, but it does not influence the self-weight of the structure. This force was balanced previously to the impact on the structure.

Note that dissipative forces, represented as a viscous damper in Fig 9 (constant C is the viscous damping coefficient), are neglected due to the fact that the impact occurs so fast that structural damping has no time to develop significantly.

Also note that it is not necessary consider gravitational acceleration in the mass of the structure due to the fact the structure is balanced prior to the collision. Impact results should be added to the state prior to the impact to obtain the final solution.

$$D_p(t) = V_{p,\,0}t - \int_0^t \int \frac{F(t)}{M_p} d\tau\, dt + \int_0^t \int g\; d\tau dt \tag{1}$$

$$D_s(t) = \int \int_0^t \frac{F(t) - K_s(D_s(t))}{M_s} d\tau\, dt \tag{2}$$

By developing the following change of variable, $\frac{d^4y}{dt^4} = F(t)$, and operating on Eqs. (1) and (2), as can be verified in [35], Eq. (3) is obtained.

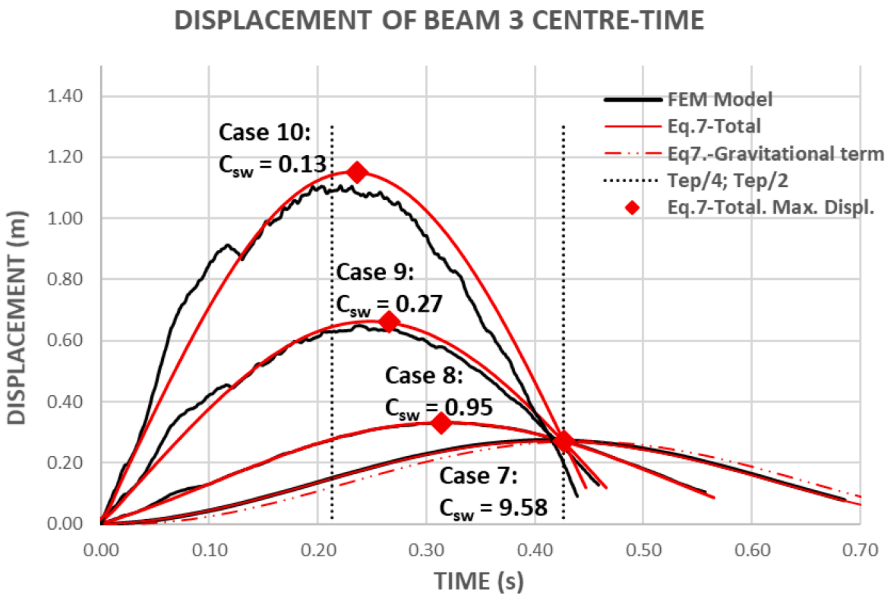

Fig. 16. Combined visualization of cases of beam 3: Cases 7–10.

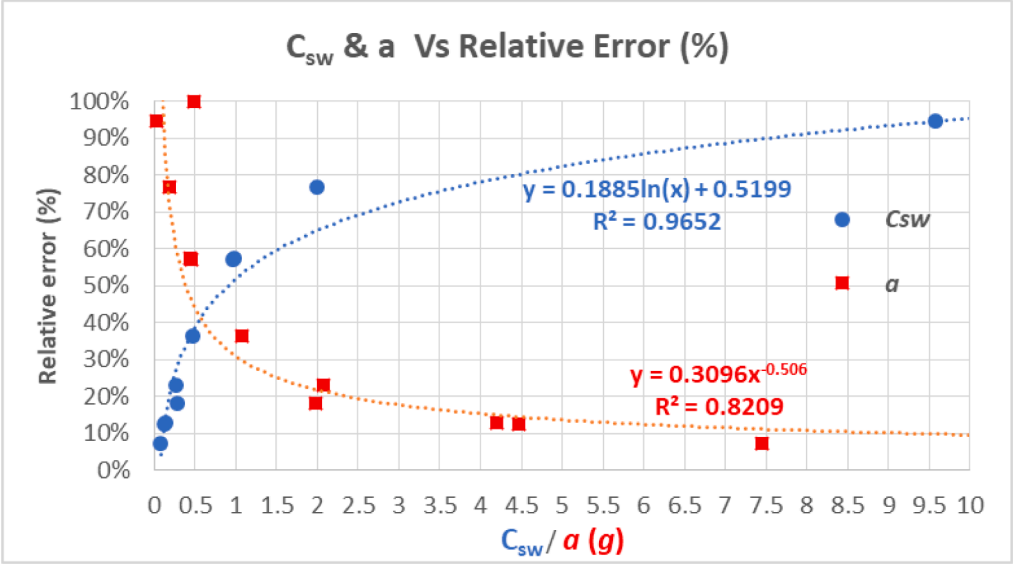

Fig. 17. Relative error due to neglecting the gravitational force in impacts versus self-weight coefficient (C_{sw}) and versus average acceleration of the structure (a).

Table 4
Maximum displacement from kinetic term, A_{k_max}, and in total, $D(s)_{max}$, according to Eq. (7) when calculating the relative error due to neglecting the gravitational force in impacts. Average acceleration a in each impact from t_0 to t_f..

Case	C_{sw}	$A_{k,max}$	$D(s)_{max}$	Relative error	t_f	a (g)
1	∞	0.00E+00	7.40e-2	100.0%	2.05e-1	0.49
2	0.98	3.77E-02	8.90e-2	57.6%	1.53e-1	0.44
3	0.47	7.88E-02	1.24e-1	36.5%	1.31e-1	1.07
4	0.28	4.08E-03	5.00e-3	18.3%	2.22e-2	1.98
5	0.14	8.06E-03	9.26e-3	13.0%	2.07e-2	4.20
6	0.08	1.39E-02	1.50e-2	7.4%	2.01e-2	7.45
7	9.58	1.42E-02	2.72e-1	94.8%	4.13e-1	0.03
8	0.96	1.43E-01	3.32e-1	57.1%	3.14e-1	0.45
9	0.27	5.09E-01	6.62e-1	23.1%	2.45e-1	2.08
10	0.13	1.01E+00	1.15e+0	12.5%	2.26e-1	4.47
11	2.00	1.84E-02	7.85e-2	76.6%	1.73e-1	0.18

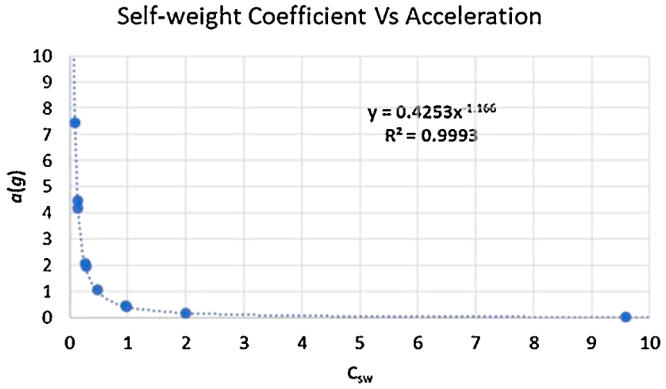

Fig. 18. Relationship between the average acceleration of the structure (a) during an impact and the self-weight coefficient (C_{sw}).

$$\ddot{y} + W_{sp}^2 y = \frac{M_s M_p}{M_s + M_p} \frac{K_s}{6M_s} V_{p,o} t^3 + \frac{M_s M_p}{M_s + M_p} V_{p,o}\, t + \frac{g\, t^4 K_s}{24 M_s} \frac{M_s M_p}{M_s + M_p} + \frac{1}{2} g\, t^2 \frac{M_s M_p}{M_s + M_p} \tag{3}$$

Where W_{sp} is the vibration frequency during the impact, which is related to the effective stiffness, K_s, equivalent mass, M_s, and projectile mass, M_p, as Eq. (4) expresses.

$$W_{sp}^2 = \frac{K_s}{M_s + M_p} \tag{4}$$

Eq. (5) shows the natural vibration frequency of the structure W_s before the impact.

$$W_s^2 = \frac{K_s}{M_s} \tag{5}$$

Meaning that, based on Eq. (4), the frequency of vibration during the impact includes the projectile mass as part of the mass of the structure

3.2.1. Problem solution

The general solution of Eq. (3) can be found as the sum of the particular solution and the homogeneous one (solution details in [35]), applying the corresponding boundary conditions. The first boundary condition results from setting the impact force null at $t = t_0$. The second boundary condition results from attributing an initial velocity V_I, immediately after the impact, Eq. (6). This boundary condition was validated in [34].

$$V_p(t=0) = V_I = V_{p,0} \frac{M_p}{M_p + M_s} \tag{6}$$

The displacement of the structure and projectile, Eq. (7), and the contact force, Eq. (8), can be calculated after applying the previous boundary conditions (the whole development can be consulted in [35]).

$$D_p(t) = D_s(t) = \frac{V_{p,0} \frac{M_p}{M_p + M_s} \sin(W_{sp}\, t)}{W_{sp}} + \frac{g M_p}{K_s} \left(1 - \cos(w_{sp}\, t)\right) \tag{7}$$

$$F(t) = M_p W_{sp} V_{p,0} \frac{M_p}{M_p + M_s} \sin(W_{sp}\, t) + g\, M_p \left(1 - \frac{M_p}{M_s + M_p} \cos(w_{sp}\, t)\right) \tag{8}$$

The first term of both Eqs. (7) and (8), is called the kinetic term (A_k) because it depends on the velocity of the projectile, while the second component of both equations is called the gravitational term (A_g), since it is influenced by the acceleration due to gravity g. The kinetic term reaches its maximum value at $T_{sp}/4$ (where T_{sp} is the vibration period during impact associated with the frequency W_{sp}) and the gravitational term reaches its maximum value at $T_{sp}/2$. In general, therefore, the maximum values of displacement and contact force will occur at a time t_f such that $\frac{T_{sp}}{4} < t_f < \frac{T_{sp}}{2}$. How closely it approaches one of these limits will depend on the relative weight of the kinetic and gravitational terms in each case. The instant t where the maximum displacements and force occur also coincides with the instant when the projectile comes to rest. The relative weight of each term will also determine the shape of the displacement-time response. When the gravitational term predominates, the curve will look more like a curve with zero initial slope, while in the case where the kinetic term predominates, the curve will be more similar to a curve with initial slope tending to V_I. The value of amplitudes of both terms in Eq. (7) at $\frac{T_{sp}}{4}$, kinetic term $A_{K,\ \frac{T_{sp}}{4}}$ and gravitational term $A_{G,\ \frac{T_{sp}}{4}}$, can be compared to obtain a self-weight coefficient. This coefficient, prior to any calculation, indicates whether the self-weight will have an influence on the final result or not. Thus, in Eq. (9) the self-weight coefficient C_{sw} is defined.

$$C_{sw} = \frac{A_{G,\ \frac{T_{sp}}{4}}}{A_{K,\ \frac{T_{sp}}{4}}} = \frac{\frac{gM_p}{K_s}}{\frac{V_{p,0} \frac{M_p}{M_p + M_s}}{W_{sp}}} = \frac{g}{V_{p,0}\ W_{sp}} \tag{9}$$

Based on Eq. (9) it can be concluded that the self-weight will influence the structural response when the impact velocity is low and when the structure is flexible (small value of W_{sp}). As can be seen in Fig. 9, a value of $C_{sw} = 0.5$ indicates at $\frac{T_{sp}}{4}$ that the gravitational term is half the Kinetic term. However, the amplitude of gravitational term ($A_{G,\ \frac{T_{sp}}{2}}$) at $\frac{T_{sp}}{2}$ is double the amplitude ($A_{G,\ \frac{T_{sp}}{4}}$) at $\frac{T_{sp}}{4}$. Therefore a $C_{sw} = 0.5$ indicates that the gravitational term has the same influence on the impact as the kinetic term, from a general point of view. Consequently, values of $C_{sw} < 0.5$ indicate that the kinetic term is dominant and values of $C_{sw} > 0.5$ indicate that gravitational term is dominant. To understand the self-weight coefficient in a simple way it should be considered that the multiplication $V_{p,0}\ W_{sp}$ ($= 2\Pi \frac{V_{p,o}}{T_{sp}}$) considers the average of the acceleration of the structure in a period. Thus, the self-weight coefficient approximates the ratio between the gravitational acceleration (g) and the average acceleration of the impact (a). When this acceleration is greater than g (e.g. >10 g), it is not necessary to consider the gravitational effect in the calculations. In any case, this limit will be discussed in detail below.

At $t > t_f$, the movement of the structure changes to the opposite direction (see Fig. 9) and the recovery phase begins, returning to its initial position. As for the projectile, either contact with the structure remains or it does not. If the former happens, that means the recovery movement of the structure is quick enough to maintain the contact, pushing the projectile in the opposite direction to the one the system had until t_f. The latter will occur if the recovery movement is not quick enough, or if the projectile falls laterally or breaks, losing contact with the structure. At $t > t_f$ Eqs. (7) and (8) remain valid in the scenario in which the projectile and the structure remain in contact during recovery time. Otherwise, the assumptions about the impact would be different. In general, the time for impact analysis is restricted to $t \leq t_f$, as the maximum displacement and maximum force on the structure are given within this time period.

The α parameter defines the relevance of higher modes of vibration [34] in the structural response. Thus, α defines whether the structure (beams, plates, frames, etc.) can be simplified to its fundamental mode with enough accuracy. The main conclusion shown in [34] in this regard is that if $\alpha > 1$, the fundamental mode always absorbs more than 50% of energy impact. The larger α is, the more energy is absorbed by the fundamental mode. Based on these key points, the limits of the application of the proposed formulation are the following:

- $\alpha > 1$ to apply in bending moments due to equivalent static force and displacements.
- $\alpha > 3$ to apply in shear forces due to equivalent static force and contact force.

Note that contact force is the 4th derivative of the function solved, while displacement is the 2nd. This is the reason why a higher value of α is needed to calculate the shear forces and contact forces.

The last consideration in the theoretical basis of the proposed simplified model is that the parameters of the structure defining the fundamental mode K_s have been considered to be elastic for the sake of simplicity of the laboratory test. If the secant line in the stress-strain curve of the material is considered, the inelastic behaviour of the structure can also be modelled with the proposed formulation in an iterative process.

3.3. Description of the measurement system in experimental tests

The measuring equipment used for the tests and for the calibration of sensors consisted of NI-PXIe 1078Data acquisition equipment, Fig. 3a

connected to a data display screen which provided real-time data visualisation, including vibration frequencies, Fig. 3b.

The system also included a power supply which provided the ±5 V voltage for the Potentiometer Displacement Transducer Unit and an APC Back-UPS ES 700 Uninterruptible Power Supply (UPS). The UPS, in addition to providing power in the event of a power failure during the test, was responsible for eliminating a possible peak voltage from the electric current. A bidirectional 120 Ω Tokyo Sokki FCA-3–11–1L strain-gauge, Fig. 4, was used as a sensor, which consisted of 2 strain gauges perpendicular to each other. The strain at the point of the structure under study was recorded by the strain gauge orientated along the longitudinal axis of the beam. The strain-gauge orientated in the transverse direction was intended to eliminate the effects due to thermal increases.

A Potentiometer Displacement Transducer Unit (PDTU), Fig. 5, was used as a sensor for measuring displacements up to one hundredth of a millimetre. It was used for calibration of the strain-gauge. The software used for the development of the measurement and data processing programs was Labview (National Instruments).

In the dynamic test, it was not possible to use the PDTU because of the high friction it introduced into the system. For this reason, a static test was carried out with the PDTU in order to calibrate the strain-gauge. The use of strain-gauges calibrated under static conditions to infer a midspan vertical displacement under impact load was considered adequate due to the fact that all impacts in this paper have an α coefficient (M_p/M_e) >>1. This value of the parameter ensured that the first mode would be the main mode involved in the impact in energetic terms [34], so the relationship between strain and midspan vertical displacement could be established. The increments in the strain-gauge related to the increments in the displacement at the centre of the beam were correlated for mode 1, Fig. 6 left, and mode 3, Fig. 6 right. Thus, the correlation between the strain measured by the strain-gauge and the experimental displacement at the centre of the beam obtained in the static test provided the displacement in the dynamic test, where only the strain-gauge was present.

The strain-gauge was placed at the centre of the span of each beam, on the underside to avoid damage during the tests. For the dynamic tests, data were recorded at a frequency of 1000 Hz in order to characterise the dynamic behaviour of the structure with sufficient accuracy. All sensor cable connections were tinned and insulated with heat-shrunk sleeves to improve the accuracy of the system and stabilise the measurement. The strain gauges were connected in a half Wheatstone bridge.

4. Results

From the impact values (equivalent stiffness, equivalent masses, etc.) previously calculated, Table 1, and through Eq. (7), the maximum displacements of the structure $D_s(t)$ are summarized in Table 3 for the ten impact cases studied, and compared with the Experimental Test /FEM model results.

In the following, all the graphs of results are presented. The experimental test results are shown in blue, the FEM model results are shown by a black line and the total results of the proposed formulation Eq. (7) are shown by a solid red line. The two terms of Eq. (7) that make up the total solution, i.e. the kinetic term (dashed red line) and the gravitational term (dashed-dotted red line) are also shown to enable the analysis of the influence of each term. The results of the first 3 tests on beam 1 (3 mm depth) are shown in Fig. 10. It can be stated that the results obtained from Eq. (7) for beam 1 agree quite well with both the results obtained from the finite element model and the experimental test results, which are very close to each other.

The three tests on beam 2, 12 mm depth, stiffer than the previous one, are shown in Fig. 11.

The results for beam 2, both in terms of the experimental test results and those from the FEM model, are in good agreement with the proposed formulation. In the experimental results (as also happened with beam 1, but to a slightly lesser extent than with beam 2 because the value of α is double in beam 1) the contribution of modes other than the fundamental mode is clearly observed. The formulation involves only the fundamental mode and therefore does not perfectly fit all the small oscillations that occur on the main wave. Due to the fact that all impacts analysed in this research have $\alpha > 1$ (see Table 1), it can be assumed that the fundamental mode is the main mode in terms of impact energy absorption [35]. This is why, even though the contributions of higher modes of vibration have not been not considered, the results are quite convergent between the proposed formulation, the FEM models and the laboratory tests. Once it was verified that the results of the FEM models and those of the experimental tests match well, a new FEM model is used to perform the analysis of a beam of larger dimensions, beam 3, to compare the results of the proposed formulation with a FEM model for a beam of more common dimensions in civil engineering. The results of beam 3 are shown in Fig. 12. It can be concluded that there is also good agreement between the FEM results and the proposed formulation for a beam of larger dimensions.

Both displacements and contact force are shown in the results of case 11, Fig. 13. Case 11 has a self-weight coefficient of $C_{sw} = 2$, so the gravitational term is the main term in the column response. Regarding contact force, FEM model results show the influence of higher modes of vibration with a small wave on the main wave, but the proposed formulation fits very well with both the maximum contact force and also the time when it happened. The large α parameter value in this case (α=10) makes the influence of higher modes of vibration relatively small.

5. Discussion

In Eq. (9), the value of the self-weight coefficient is established, which enables the importance of the gravitational force in the final deformation to be appreciated. In this section, this coefficient is analysed for the different tests carried out in this article. The results for each beam are shown together to better illustrate the variation in structural response. In each of the graphs, the gravitational term in the response of each beam is presented, as it is common to all the tests of that beam, since the mass of the projectile is constant for each beam. The kinetic term is not presented to avoid superimposing too many curves, since it is the variable term in the tests (depending on the height of the projectile drop). This term, added to the gravity term, gives the overall structural response, Eq. (7).

In Fig. 14, all the results of tests performed on beam 1 are shown together (cases 1, 2 and 3). In case 1, where the self-weight coefficient is infinite, see Table 3, because the drop velocity is zero (projectile glued to the beam), the gravitational term is superimposed on the total value of Eq. (7). For this case, the curves, both in the experimental results and in the proposed formulation, present a zero initial tangent and the maximum deformation occurs for exactly $T_{sp}/2$. However case 3 clearly presents a non-zero initial tangent, characteristic of the contribution of the kinetic term, and the maximum deformation occurs for an intermediate value between $\frac{T_{sp}}{4}$ and $\frac{T_{sp}}{2}$.

In the tests on beam 2, which is stiffer than beam 1, the values of the coefficient C_{sw} are smaller as can be seen in Table 3 and Fig. 15. This is because in stiff structures the gravity factor has less influence, as can be verified in Eq. (9), due to the parameter of vibration frequency of the structure during impact (W_{sp}). Consequently, the values of all the C_{sw} coefficients are clearly less than 0.5 for this beam and, therefore, all the curves have a non-zero initial slope that clearly approaches the value of the initial tangent of the kinetic term in each case (V_I) when the C_{sw} coefficient approaches zero. Likewise, as was previously stated, when this coefficient decreases, the kinetic term dominates and therefore the time at which the maximum displacement occurs approaches $T_{sp}/4$.

The trend described in the laboratory tests for beams 1 and 2 is

similar for beam 3. For case 7, as can be seen in Fig. 16, the value of C_{sw} is clearly above 0.5 (9.58), Table 3. This means that the structural response is dominated by the gravitational term, and as a consequence the curve has practically zero initial tangent, with a maximum displacement time very close to $T_{sp}/2$. However, Case 10 shows a $C_{sw} =$ 0.13 which, being much smaller than 0.5, indicates that the kinetic term dominates, and therefore the curve has an initial tangent close to V_I and a maximum displacement time close to $T_{sp}/4$. The value of C_{sw} represents the ratio of amplitudes between the gravitational term and the kinetic term at the instant of time equal to $T_{sp}/4$, so that in case 10, which is dominated by the kinetic term, it can be said that the gravitational term represents approximately about 13% of the total at the instant of maximum displacement. Cases 8 and 9 are intermediate cases showing the evolution from one case to the other of the previously explained extreme cases, cases 7 and case 10.

Fig. 17 depicts the relative error considering only the kinetic term Eq. (7) versus the self-weight coefficient C_{sw}. The relative error was calculated from the ratio between maximum displacement considering only the kinetic term and the maximum displacement considering both the kinetic and the gravitational terms. Numerical results are shown in Table (4). Thus, Fig. 17 shows the error due to neglecting the gravitational force in the calculations of impacts. Fig. 17 also shows the relative error versus the average acceleration (a) of the structure at each impact. The parameter a was calculated according to the expression $a = \mathrm{D_s(t)_{max.\,Eq(7)}}/\mathrm{t_f}$. The numerical results are shown in Table (4).

It can be concluded based on Fig. 17 that the relative error due to neglecting gravitational force decreases as the average acceleration (a) increases. Similarly, this relative error increases if the self-weight coefficient C_{sw} increases. This is because parameter $\mathrm{C_{sw}}$ is related to the ratio between the gravitational acceleration and the average acceleration of the structure. To verify this idea, numerical results of parameter a and $\mathrm{C_{sw}}$ shown in Table 4 are related in Fig. 18.

Consequently, and based on results shown in Fig. 17, if an acceleration in an impact (a) is greater than 10 g the relative error due to neglecting the influence of gravity is lower than 10%. Fig. 18 shows the accuracy relationship between parameters C_{sw} and a ($R^2 = 0.9993$). Therefore, based on Figs. 17 and 18, in order to ensure an error lower than 10% in the displacement, a value of C_{sw} lower than 0.1 is required. Otherwise, gravitational force should be considered in impact calculations to avoid this error. Thus finally, based on the previous analysis it makes sense to use the equations from the proposed simplified method to considerer the gravitational influence when the acceleration during impact is in the range between 0 and 10 g, and this can be ensured if $\mathrm{C_{sw}}$ is lower than 0.1.

6. Conclusions

The proposed formulation with the 1-DoF System fits quite well with both the results of the FEM model and those of the experimental tests on the displacement of the structure. Regarding the contact forces, due to the limitations inherent to FEM models, it has not been possible to verify them in transverse impacts with the proposed formulation. Only in a case with a longitudinal impact, where the FEM models are more accurate, was it possible to compare with the proposed formulation with good results. Due to that, further research would be needed to confirm that the proposed formulation predicts the contact force correctly in a general way.

The formulation states that, if the impact occurs in the direction of gravity, it is influenced by gravity in both the displacement of the structure Eq. (7) and the contact force Eq. (8). The formulation states that, for a given projectile mass, the structural response is the sum of a kinetic term, which depends on the impact velocity, and a gravitational term, which is constant for that mass. Therefore, as the impact velocity (the height of fall) increases, the gravitational term becomes less important than the kinetic term. The formulation has been shown to fit the test results very accurately, irrespective of the importance of the two terms in each case. The research results show that large accelerations enable the effect of gravitational acceleration to be neglected. In order to evaluate in advance whether it makes sense to consider the effect of gravity in an impact, a self-weight coefficient, C_{sw} Eq. (9), has been proposed. A reliable relationship has been found between C_{sw} and the average acceleration of the structure (a) during the impact. Thus, with this basis, a value of C_{sw} lower than 0.1 ensures a large average acceleration of the structure (greater than 10 g), and therefore the gravitational influence on impacts can be neglected because the relative error is lower than 10%. Consequently, outside this range the proposed equations no longer make sense for use in analysing gravitational influence. This coefficient C_{sw} is the ratio between the amplitude of the gravitational term and the kinetic term at instant $\frac{T_{sp}}{4}$. Values close to or above 0.5 indicate that the gravitational term has a large influence on the structural response and values clearly below 0.5 indicate a small influence. For small values of C_{sw}, the value of the coefficient itself approximates to the proportion of the gravity term in the maximum deformation of the structure. It has also been verified when testing two beams of equal length, but different depths, that C_{sw} also indicates that more rigid structures are less affected by gravity than flexible ones.

Based on the Self-Weight Coefficient C_{sw}, the engineer performing the calculations will be able to decide whether considering the force of gravity is meaningful, and if not, that C_{sw} indicates the error induced in calculations due to neglecting the gravitational force.

The limits of applicability of the proposed formulation were stated in [34] depending on the α parameter.

The impact behaviour is certainly complex and it might seem that the hypotheses are simplistic, however research shows what is essential about impacts, which is novel and very difficult to achieve. It shows when and why different modes are activated, when the gravity force needs to be considered in calculations, and how and why the natural frequency of the structure is modified during impact. Additionally, from a design engineering viewpoint, the research elucidates the expected displacement and the expected contact force in an impact with any structure thus permitting the pre-design and verification of results obtained by means of complex FEM models. These conclusions were obtained thanks to the simplifications undertaken.

CRediT authorship contribution statement

Javier Sánchez-Haro: Conceptualization, Methodology, Investigation, Formal analysis, Data curation, Writing – original draft. **Ignacio Lombillo:** Conceptualization, Methodology, Validation, Writing – review & editing, Supervision. **Guillermo Capellán:** Resources, Validation, Writing – review & editing.

Declaration of Competing Interest

The authors declare that they have no known competing financial interests or personal relationships that could have appeared to influence the work reported in this paper.

Data availability

Data will be made available on request.

Acknowledgements

We would like to thank *Simulsoft Ingenieros España* for lending the Midas NFX software for use in this research, which has been of great help. There are not many companies that share their resources with the academic world in a disinterested way and, therefore, we greatly appreciate their commitment to research and training of future

engineers.

References

[1] Goldsmith W. Impact. Courier Corporation; 2001.
[2] Stronge WJ. Impact mechanics. Cambridge University Press; 2018.
[3] Jelinek JJ. Impact of a mass on a beam. University of California, Berkeley; 1943.
[4] R. Alverson, "Impact with finite acceleration time of elastic and elastic-plastic beams," 1956, Accessed: Jul. 28, 2021. [Online]. Available: https://asmedigitalcollection.asme.org/appliedmechanics/article-abstract/23/3/411/1110633.
[5] T Z, N M. On the impacts of beams. Inst Phys Chem Res 1938;826.
[6] B. de Saint-Venant, "Theorie de plasticité de corps solide de Clebsch," Paris, Fr., 1883.
[7] Hertz H. Über die berührung fester elastischer körper. J für die reine und Angew Math 1882;92(156–171):22.
[8] Timoshenko SP. Zur frage nach der wirkung eines stosses auf einen balken. Z Angew Math Phys 1913;62(1–4):198–209.
[9] Lennertz J. Beitrag zur frage nach der wirkung eines querstoßes auf einen stab. Arch Appl Mech 1937;8(1):37–46.
[10] Eringen AC. The transverse impact on beams and plates. ASME J Appl Mech 1953;20:461.
[11] Lee EH. The impact of a mass striking a beam. Trans Am Soc Mech Eng 1940;A-129:62.
[12] Lee Y, Hamilton JF, Sullivan JW. The lumped parameter method for elastic impact problems. Appl Mech 1983. https://doi.org/10.1115/1.3167152.
[13] Suaris W, Shah SP. Inertial effects in the instrumented impact testing of cementitious composites. Cem Concr Aggregates 1981;3(2):77–83.
[14] Shivakumar KN, Elber W, Illg W. Prediction of impact force and duration due to low-velocity impact on circular composite laminates. Appl Mech 1985. https://doi.org/10.1115/1.3169120.
[15] Yang Y, Lam NTK, Zhang L. Estimation of response of plate structure subject to low velocitiy impact by a solid object. Int J Struct Stab Dyn 2012;12(06):1250053. https://doi.org/10.1142/S0219455412500538. Dec.
[16] Yang Y, Lam NTK, Zhang L. Evaluation of simplified methods of estimating beam responses to impact. Int J Struct Stab Dyn 2012;12(3):1250016. https://doi.org/10.1142/S0219455412500162.
[17] Lam NTK, Tsang HH, Gad EF. Simulations of response to low velocity impact by spreadsheet. Int J Struct Stab Dyn 2010;10(3):483–99. https://doi.org/10.1142/S0219455410003580.
[18] Shi S, Zhu L, Yu TX. Dynamic modelling of elastic-plastic beams under impact. Int J Impact Eng 2019;126:1–10. https://doi.org/10.1016/j.ijimpeng.2018.11.017.
[19] Hao Q, et al. Transient impact analysis of elastic-plastic beam with strain-rate sensitivity. Int J Impact Eng 2021;153:103865. https://doi.org/10.1016/j.ijimpeng.2021.103865.
[20] Ugrimov SV, Shupikov AN, Lytvynov LA, Yareshchenko VG. Non-stationary response of sapphire rod on longitudinal impact. Theory and experiment. Int J Impact Eng 2017;104:55–63. https://doi.org/10.1016/j.ijimpeng.2017.02.005.
[21] Idesman AV, Mates SP. Accurate finite element simulation and experimental study of elastic wave propagation in a long cylinder under impact loading. Int J Impact Eng 2014;71:1–16. https://doi.org/10.1016/j.ijimpeng.2014.04.002.
[22] Fíla T, et al. Dynamic impact testing of cellular solids and lattice structures: application of two-sided direct impact Hopkinson bar. Int J Impact Eng 2021;148:103767. https://doi.org/10.1016/j.ijimpeng.2020.103767.
[23] Bassi A, Genna F, Symonds PS. Anomalous elastic–plastic responses to short pulse loading of circular plates. Int J Impact Eng 2003;28(1):65–91. https://doi.org/10.1016/S0734-743X(02)00036-2.
[24] Smetankina NV, Shupikov AN, Sotrikhin SY, Yareschenko VG. Dynamic response of an elliptic plate to impact loading: theory and experiment. Int J Impact Eng 2007;34(2):264–76. https://doi.org/10.1016/j.ijimpeng.2005.07.016.
[25] Wu XQ, Zhong B, Lv Y, Li ZX, Chouw N. Experimental study on dynamic amplification factor of simple-supported reinforced concrete beams under impact loading generated by an impulse hammer. Int J Struct Stab Dyn 2021;21(3):2150036. https://doi.org/10.1142/S021945542150036X.
[26] Anil Ö, Durucan C, Erdem RT, Yorgancilar MA. Experimental and numerical investigation of reinforced concrete beams with variable material properties under impact loading. Constr Build Mater 2016;125:94–104. https://doi.org/10.1016/j.conbuildmat.2016.08.028.
[27] Chen W, Pham TM, Elchalakani M, Li H, Hao H, Chen L. Experimental and numerical study of basalt FRP strip strengthened RC slabs under impact loads. Int J Struct Stab Dyn 2020;20(6):2040001. https://doi.org/10.1142/S0219455420400015.
[28] Ávila de Oliveira L, Luiz Passaia Tonatto M, Luiza Cota Coura G, Teixeira Santos Freire R, Panzera THallak, Scarpa F. Experimental and numerical assessment of sustainable bamboo core sandwich panels under low-velocity impact. Constr Build Mater 2021;292:123437. https://doi.org/10.1016/j.conbuildmat.2021.123437.
[29] Daneshvar K, Moradi MJ, Ahmadi K, Hajiloo H. Strengthening of corroded reinforced concrete slabs under multi-impact loading: experimental results and numerical analysis. Constr Build Mater 2021;284:122650. https://doi.org/10.1016/j.conbuildmat.2021.122650.
[30] D'Antimo M, Latour M, Rizzano G, Demonceau J-F. Experimental and numerical assessment of steel beams under impact loadings. J Constr Steel Res 2019;158:230–47.
[31] Li H, Chen W, Pham TM, Hao H. Analytical and numerical studies on impact force profile of RC beam under drop weight impact. Int J Impact Eng 2021;147:103743.
[32] Madjlessi N, Cotsovos DM, Moatamedi M. Drop-weight testing of slender reinforced concrete beams. Struct Concr 2021.
[33] Yu Y, Lee S, Cho J-Y. Deflection of reinforced concrete beam under low-velocity impact loads. Int J Impact Eng 2021;154:103878.
[34] Sanchez-Haro J, Lombillo I, Capellán G. Equivalent static force in heavy mass impacts on structures. Struct Stab Dyn 2021. https://doi.org/10.1142/S0219455422500250.
[35] Sanchez-Haro J. Development of theory on impacts. Simplified method of calculation of impacts in structures. University of Cantabria; 2017. PhD Thesis.
[36] Samartin A, Diaz del Valle J. Analysis of plate bending by means of high order finite hyperelements. Eng Struct 1986;8(1):29–38. https://doi.org/10.1016/0141-0296(86)90017-9. Jan.
[37] Man H, Song C, Xiang T, Gao W, Tin-Loi F. High-order plate bending analysis based on the scaled boundary finite element method. Int J Numer Methods Eng 2013;95(4):331–60. https://doi.org/10.1002/NME.4519. Jul.